

# Robust Input Shaping for Sway Control of an Overhead 3D Crane

A. M. Abdullahi<sup>1,2</sup>, Z. Mohamed<sup>1</sup>, H. Selamat<sup>1</sup>, M.S. Zainal Abidin<sup>1</sup>,  
A. Haruna<sup>1,2</sup>, L. Ramli<sup>1</sup>, A. A. Bature<sup>1,2</sup>

<sup>1</sup>Faculty of Electrical Engineering, Universiti Teknologi Malaysia, 81310 Johor Bahru, Johor, Malaysia.

<sup>2</sup>Department of Mechatronics Engineering, Faculty of Electrical, Bayero University Kano 3011, Nigeria.  
auwal@fkegraduate.utm.my

**Abstract**—This paper presents a robust input shaping control of an overhead 3D crane. Control of a crane in the presence of wind disturbance during payload hoisting is extremely challenging, as hoisting with wind disturbance causes high unwanted payload sway, which makes payload positioning difficult to achieve. Two robust input shaping techniques are presented, the zero vibration derivative-derivative (ZVDD) and extra insensitive (EI) shapers. Simulations using a nonlinear 3D overhead crane model were performed and the performances of the two robust input shapers are compared. In these investigations a wind disturbance force of magnitude 0.3 N is considered for the robustness test, in addition different payload mass were tested. It is predicted that the method can be very useful in reducing the complexity of closed-loop controllers for both tracking and sway control.

**Index Terms**—3D Overhead Crane; Hoisting; Payload Sway; Robust Shaper; Wind Disturbance.

## I. INTRODUCTION

A crane system is an industrial machine commonly used in factories and seaports for loading and unloading heavy loaded containers. Crane operations are required to be as fast as possible with a higher rate of load positioning accuracy. Payload hoisting is another vital aspect of crane maneuvering. However, hoisting generates unwanted crane motions such as load bouncing, twisting and swinging. These unwanted motions affect a payload's positioning precision and thus decreases an overall crane's performance [1]. The oscillation control of a suspended load, such as in a three-dimensional space (3D) crane has been an interesting field of research. The force of inertia that acts on the load when a command signal is injected on the crane causes a high amplitude oscillation in the payload's sway motion [2]. However, in most cases the presented control schemes were not suitable for real time applications. Therefore, the crane operation is not automatic and continuously requires an operator to monitor the crane during operation, and most of the times, the operator has not been able to compensate for the unwanted payload sway motion [3]. Another unavoidable problem in crane control is the presence of disturbance signals due to model uncertainties or external influences such as wind motion. To achieve a smooth crane operation in this situation, a robust control is required for rejection of the disturbances.

Investigations have shown that the control of crane systems can be classified into feedforward and feedback control strategies. A feedforward control alters the command input signal to cancel the system's oscillation, while a feedback control estimates the system's states in order to reduce the effect of the unwanted oscillation [4]. A number of feedforward controls have been developed using Finite Impulse Response (FIR) filters for vibration control of several systems. These include a direct method of an adaptive FIR filter [5], a quadratic FIR filter [6] and a multi-input multi-output FIR feedforward filter for tracking control [7]. Furthermore, a digital shaping filter has also been proposed for reducing machine vibration [8] and a time-delay pre-filter for vibration control [9]. One of the practical and effective feedforward controllers is using an input shaping approach, and the approach has been widely used by many researchers for control of the residual vibration of flexible structures [10]. By using this technique, system vibration is reduced by convolving a command input signal with a sequence of impulses that are designed based upon natural frequencies and the damping ratios of the system. The earliest input shaping approach was introduced in [11]. Since then, several modified input shaping techniques have been designed and implemented on various systems. These includes a vector diagram approach input shaping [12], finite-state input shaping [13], extra-intensive shaper [14] and an input shaper designed with a distributed delay [15]. These techniques have been applied on several systems which include a 3D crane [16] and a very flexible manipulator system [17], recently an output-based command shaping for sway control of a 3D crane is presented [18].

This paper presents two robust inputs shaping methods and investigated their performance using a wind disturbance force of magnitude 0.3 N injected into the system during payload hoisting. A payload hoisting operation of between 0.22 m to 0.72 m was considered and that corresponds to a decrement in the natural frequency and damping ratio of the system by 41% and 54%, respectively. In addition to investigate the performance of the two shapers different payload mass of 1 kg and 0.5 kg are used. This work was only tested in simulations using MATLAB Simulink environment and the two robust input shapers were implemented on the 3D nonlinear model of the 3D crane system. For the performance investigation two

cases were considered (1) simultaneous motion of the trolley and payload hoisting and (2) simultaneous motion of the trolley and payload hoisting in the presence of wind disturbance force of magnitude 0.3 N.

## II. DYNAMIC OF A 3D CRANE

The development of a nonlinear model of a lab scaled 3D crane as shown in Figure 1 is described in this section. The mathematical model was obtained by using the Lagrange method based upon the given characteristics of the crane by the manufacturer and study in [19]. The obtained model was simulated using MATLAB Simulink to investigate the dynamic behaviour of the system.

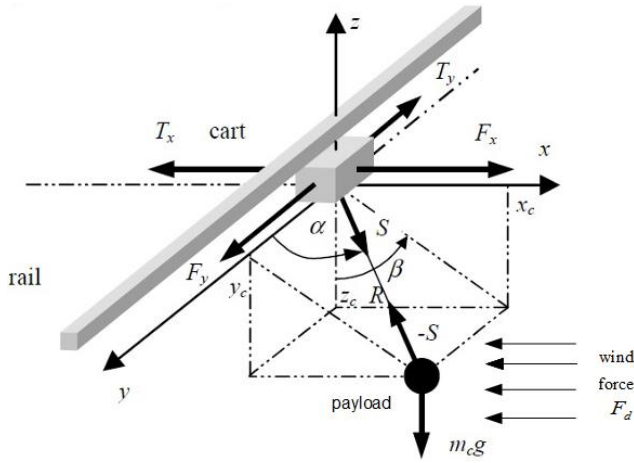


Figure 1: Schematic Diagram and Forces

A schematic diagram of the 3D crane system is shown in Figure 1 with  $XYZ$  as the coordinate system.  $\alpha$  represents the angle of the lift-line with the  $Y$  axis and  $\beta$  represents the angle between the negative part of the  $Z$  axis and the projection of the payload cable onto the  $XZ$  plane.  $T$  is the reaction force in the payload cable acting on the trolley.  $F_x$  and  $F_y$  are the forces driving the rail and the trolley, respectively.  $F_z$  is the force lifting the payload and  $f_x$ ,  $f_y$  and  $f_z$ , are the corresponding friction forces.  $m_p$ ,  $m_t$ , and  $m_r$  are the payload mass, the trolley mass (including the gear box, the encoders and the DC motor) and the moving rail, respectively, and  $l$  represents the cable length.

The equations of motion of the crane are obtained with respect to the trolley and the rail motions' coordinates  $(x, \beta, y, \alpha)$  as trolley movement, trolley sways angle, rail movement and rail sway angle respectively. With a disturbance signal  $F_d$ , the model is obtained as:

$$(m_t + m_r + m_p)\ddot{x} + m_p l \ddot{b} \cos b \cos a - m_p l \ddot{a} \sin b \sin a - m_p l \dot{b}^2 \sin b \cos a - 2m_p l \dot{a}^2 \sin b \cos a - 2m_p l \dot{b} \dot{a} \cos b \sin a = F_x - f_x \dot{x} + F_d \quad (1)$$

$$(m_r + m_p)\ddot{y} + m_p l \ddot{c} \cos a - m_p l \dot{a}^2 \sin a = F_y - f_y \dot{y} + F_d \quad (2)$$

$$m_p l^2 \ddot{b} \cos^2 a + m_p l \ddot{c} \cos b \cos a + m_p g \sin b \cos a - 2m_p l^2 \dot{b} \dot{a} \sin b \cos a = 0 \quad (3)$$

$$m_p l^2 \ddot{a} + m_p l \ddot{c} \cos a + m_p g \sin a \cos b - m_p l \ddot{b} \sin b \sin a + m_p l^2 \dot{b} \sin a \cos a = 0 \quad (4)$$

Table 1 shows the parameters of the crane used for simulation and experiment, which corresponds to the lab scale crane in Figure 1.

Table 1  
System Parameters

Symbol	Quantity
Mass of payload, $m_p$	1 kg
Mass of trolley, $m_t$	1.155 kg
Mass of moving rail, $m_r$	2.2 kg
Cable length, $l$	0.47 m
Gravitational constant, $g$	9.8 m/s <sup>2</sup>
Corresponding friction forces, $f_x, f_y, f_z$	100, 82, 75 kgm/s <sup>2</sup>
Mass of payload, $m_p$	1 kg

## III. CONTROL SCHEME

This section describes the design of the zero vibration derivative-derivative (ZVDD) and extra insensitive (EI) shapers.

### A. Design of Zero Vibration Derivative-Derivative Shaper

The design of the ZVDD shapers for the sway control of a 3D crane with hoisting is described in this section. As the system behaviour changes during the hoisting operation of between 0.22 m and 0.72 m, which corresponded to frequency changes from 6.41 Hz to 3.73 Hz respectively.

An oscillatory system can be modelled as a superposition of second order systems, each with a transfer function as:

$$G(s) = \frac{\omega_n^2}{s^2 + 2\zeta\omega_n s + \omega_n^2} \quad (5)$$

where  $\omega_n$  is the natural frequency and  $\zeta$  is the damping ratio of the system. In time domain, the response of the system can be expressed as:

$$y(t) = \frac{A\omega_n}{\sqrt{(1-\zeta^2)}} e^{-\zeta\omega_n(t-t_0)} \times \sin\left(\omega_n(t-t_0)\sqrt{(1-\zeta^2)}\right) \quad (6)$$

where  $A$  and  $t_0$  are the amplitude and time instant of the impulse respectively. By superposition, the response to an impulses sequence after the last impulse can be obtained as

$$y(t) = \sum_{k=1}^N \left[ \frac{A_k\omega_n}{\sqrt{(1-\zeta^2)}} e^{-\zeta\omega_n(t-t_k)} \right] \times \sin\left(\omega_n(t-t_k)\sqrt{(1-\zeta^2)}\right) \quad (7)$$

A residual single mode vibration amplitude of the impulse response can be obtain at the time of the last impulse  $t_k$  as:

$$V(\omega_n, \zeta) = e^{-\zeta\omega_n t_k} \sqrt{R_1^2 + R_2^2} \quad (8)$$

where

$$R_1 = \sum_{k=1}^N A_k e^{\zeta\omega_n t_k} \sin\left(\omega_n t_k \sqrt{(1-\zeta^2)}\right)$$

$$R_2 = \sum_{k=1}^N A_k e^{\zeta\omega_n t_k} \cos\left(\omega_n t_k \sqrt{(1-\zeta^2)}\right)$$

Figure 2 shows the ZVDD shaping process where  $A_k$  and  $t_k$  are the magnitudes and the locations at which the impulses occurred.  $t_k$  is the time of the  $K^{th}$  impulses and is a non-negative value, and  $A_k$  is an amplitude of the  $K^{th}$  impulse and is a non-zero value.  $t_0 = 0$  was chosen in order to avoid a response delay. With  $w_d = \omega_n \sqrt{(1-\zeta^2)}$  the ZVDD design parameters were deduced as in [20]. To obtain a similar rigid body motion of unshaped command, the sum of the shaper's amplitudes of the impulse should be unity. This gives the summation constraints as:

$$\sum_{k=1}^n A_k = 1 \quad (9)$$

ZVDD shaper's parameters can be obtain as:

$$\begin{bmatrix} A_k \\ t_k \end{bmatrix} = \begin{bmatrix} \frac{1}{(1+K)^3} & \frac{3K}{(1+K)^3} & \frac{3K^2}{(1+K)^3} & \frac{K^3}{(1+K)^3} \\ 0 & \tau_d & 2\tau_d & 3\tau_d \end{bmatrix} \quad (10)$$

where

$$\tau_d = \frac{\pi}{\omega_n \sqrt{(1-\zeta^2)}} \quad \text{and} \quad K = e^{\frac{-\pi\zeta}{\sqrt{(1-\zeta^2)}}}$$

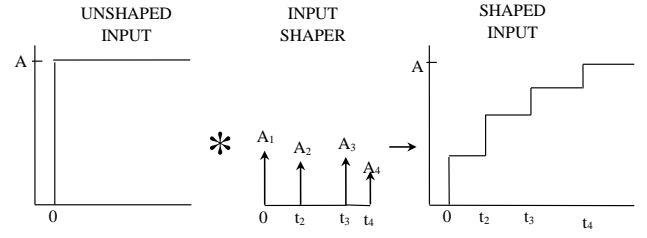


Figure 2: ZVDD Shaping Process

### B. Design of Extra Insensitive Shaper (EI)

The design of EI shaper is basically similar to the design of zero vibration (ZV) shapers such as ZVDD only that, in EI input shaping, the residual vibration  $V(\omega_n, \zeta)$  is set to nonzero value. Through relaxing zero vibration constrains to a certain value greater than zero, the robustness of input shaping can be increase. The formulation of EI shaping in this work is as derived in [14, 21] as:

$$V(\omega_n, \zeta) = V_{tol} (> 0) \quad (11)$$

where  $V_{tol} (> 0)$  is the nonzero value of the residual vibrations. The approximate numerical solution of EI for underdamped systems was obtained using optimization software with the assumption that damping ratio to be  $0 < \zeta \leq 0.3$  and the nonzero value to be  $0 \leq V_{tol} \leq 0.15$  [20] as:

$$A_1 = 0.24968 + 0.24962V_{tol} + 0.80008\zeta + 1.23328V_{tol}\zeta + 0.49599\zeta^2 + 3.17316V_{tol}\zeta^2 \quad (12)$$

$$A_2 = 1 - (A_1 + A_3) \quad (13)$$

$$A_3 = 0.25149 + 0.21474V_{tol} - 0.83249\zeta + 1.41498V_{tol}\zeta + 0.85181\zeta^2 - 4.90094V_{tol}\zeta^2 \quad (14)$$

$$t_1 = 0 \quad (15)$$

$$t_2 = (0.49990 + 0.46159V_{tol}\zeta + 4.26169V_{tol}\zeta^2 + 1.75601V_{tol}\zeta^3 + 8.57843V_{tol}^2\zeta - 108.644V_{tol}^2\zeta^2 + 336.989V_{tol}^2\zeta^3)T_d \quad (16)$$

$$t_3 = T_d = 2\pi / (\hat{\omega}\sqrt{1-\zeta^2}) \quad (17)$$

where  $\hat{\omega}$  is the modeled frequency which is assumed to have modeling error such that  $\hat{\omega} \neq \omega_n$ . It is assumed that there is error such that  $\omega_n = \hat{\omega} + \eta$  where  $\eta$  is a constant number representing the modeling error frequency value and is chosen as 0.8 Hz in this work. The parameters of the designed ZVDD and EI are given in Table 2.

Table 2  
Shaper's Parameters

Shaper	EI	ZVDD
A1 (rad)	0.2674	0.1286
A2 (rad)	0.4750	0.3785
A3 (rad)	0.2577	0.3714
A4 (rad)	-	0.1215
t1 (sec)	0	0
t2 (sec)	0.6938	0.8423
t3 (sec)	1.3870	1.6845

IV. IMPLEMENTATION AND RESULTS

This section provides the implementation of the designed ZVDD and EI shapers on the crane through simulations. A simultaneous motion of the crane trolley, and payload hoisting in the presence of wind disturbance force, which is common in industrial operation, was investigated using the shapers. Payload hoisting between 0.22 m to 0.72 m which corresponded to decrease in the system's natural frequency and damping ratio by 42% and 54%, respectively. Meanwhile the objective is to obtain a zero sway, a mean square error (MSE) might be used as a performance index, in which a small value of MSE indicates a low sway response. The performance of the input shapers was tested on the two cases as follows;

Case I:  
Simultaneous motion of the trolley and payload hoisting.

Case II:  
Simultaneous motion of the trolley and payload hoisting in the presence of wind disturbance force of magnitude 0.3 N.

In both cases different payload mass of 1 kg and 0.5 kg were tested. Figure 3 shows the control block diagram that was used for a payload sway motion control of the crane system where  $x, \beta, y, \alpha$  and  $z$  represent the trolley position, the trolley sway, the rail position, the rail sway, and the hoisting position respectively, where  $r$  is the input signal to the crane system. A pulse input signal with amplitude of 0.5 N and a width of 3 seconds was used for the simulations. Using this input signal, a suitable system response for the investigations was obtained. The control block diagram of the input shaping is as shown in Figure 3.

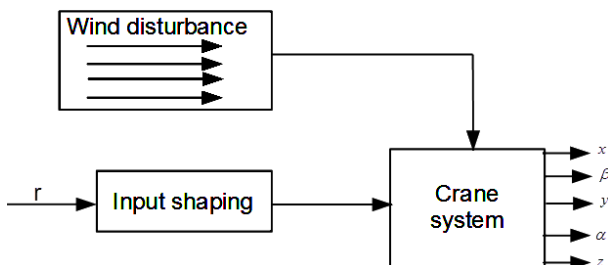


Figure 3: Control Block Diagram

A. Simulation Results

The simulations were implemented within the MATLAB simulation environment of the 3D crane system with the same parameters as the lab-scale crane. The shaped outputs of the input shapers are applied to the nonlinear crane system for the investigations of their performance. Figures 4 and 5 show the sway response of the ZVDD, and the EI, for Case I. It is noted that the maximum transient sway of the ZVDD, and EI, were 3.5836, and 3.1304 degrees, respectively, and their overall sway was measured by using MSE as 0.8696, and 0.6086, respectively. A similar pattern of results was obtained for Case II with a simultaneous movement of the trolley, and the payload hoisting in the presence of wind disturbance force of magnitude 0.3 N.

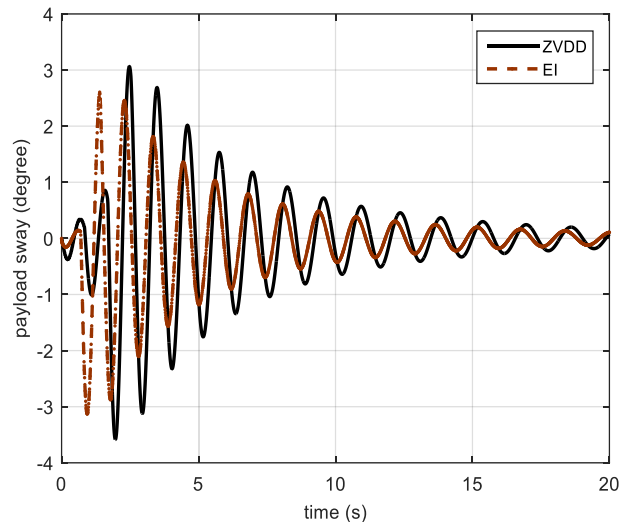


Figure 4: Payload (1 kg) sway with hoisting

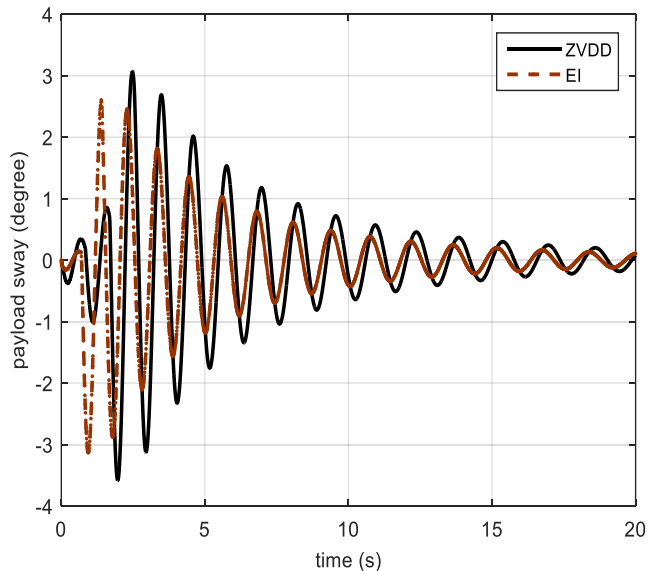


Figure 5: Payload (0.5 kg) sway with hoisting

Figures 6 and 7 show the payload sway responses using case II for the ZVDD and EI. It was observed that the EI gave the highest sway reduction when compared to the ZVDD. Tables

3 and 4 summarises the simulation results of the payload sway for both case I and case II respectively.

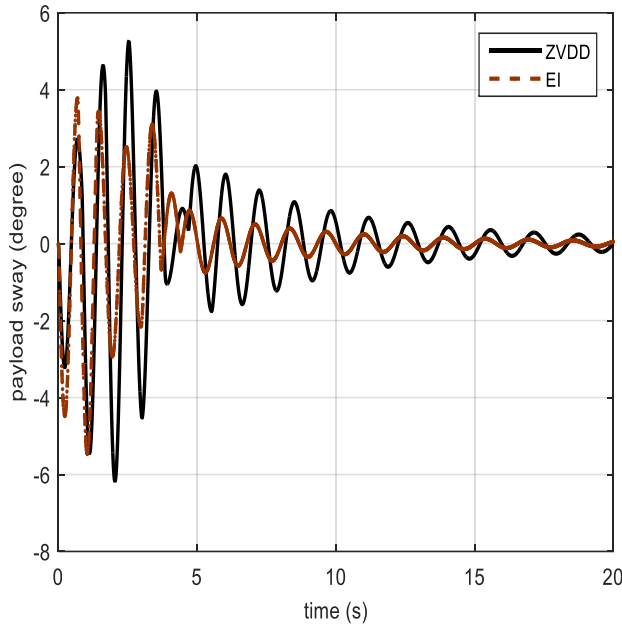


Figure 6: Payload (1 kg) sway with hoisting and disturbance

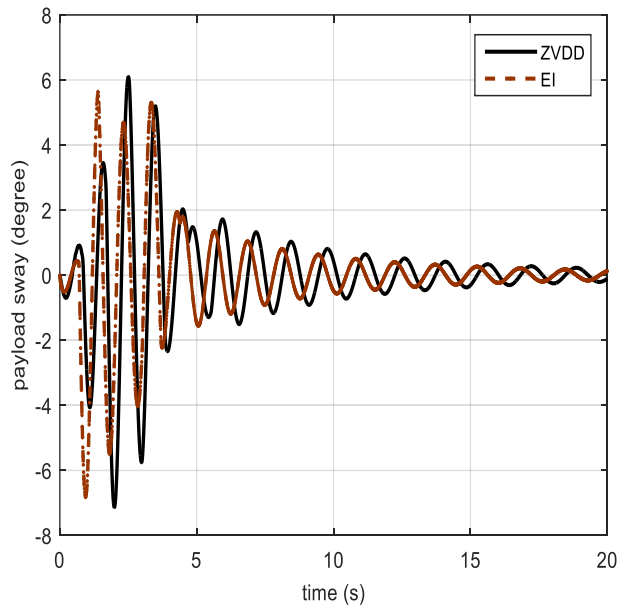


Figure 7: Payload (0.5 kg) sway with hoisting and wind disturbance

Table 3  
Performance with Payload Hoisting

Shaper	ZVDD	EI
MSE (deg)	0.8696	0.6086
MTS (deg)	3.5836	3.1304

\*MSE: Mean Square Error; MTS: Maximum Transient Sway

Table 4  
Performance with Payload Hoisting and Wind Disturbance

Shaper	ZVDD	EI
MSE (deg)	2.3952	1.2634
MTS (deg)	6.1778	5.4675

\*MSE: Mean Square Error; MTS: Maximum Transient Sway

### V. CONCLUSION

An investigation on robustness of two robust input shaping methods has been conducted. A crane is a time varying system, as the dynamic behaviour of the crane changes during the hoisting operation and with wind disturbance force. Two robustness cases were investigated based on the crane motion with hoisting only and its motion with hoisting in the presence of wind disturbance. The performance comparisons between the ZVDD and the EI shapers show that the EI gave a better sway reduction in both cases as compared to ZVDD. This is clearly shown by comparing their MSE values, it can be seen in both cases the EI has the lowest MSE which indicated better performance in the payload sways reduction.

### ACKNOWLEDGMENT

The authors would like to thank Universiti Teknologi Malaysia and the Ministry of Higher Education for their supports. This project is supported by Research University Grant Vote 13H78.

### REFERENCES

- [1] Y. Jisup, S. Nation, W. Singhose, and J. E. Vaughan, "Control of crane payloads that bounce during hoisting," *IEEE Trans. on Control Systems Technology*, vol.22, pp. 1233-1238, 2014.
- [2] Z. N. Masoud, and M. F. Daqaq, "A graphical approach to input-shaping control design for container cranes with hoist," *IEEE Trans. on Control Systems Technology*, vol. 14, pp. 1070-1077, 2006.
- [3] H. M. Omar, and A. H. Nayfeh, "Gantry cranes gain scheduling feedback control with friction compensation," *Journal of Sound and Vibration*, Vol. 281, pp. 1-20, 2005.
- [4] S. Garrido, M. Abderrahim, A. Giménez, R. Diez, and C. Balaguer, "Anti-swinging input shaping control of an automatic construction crane," *IEEE Trans. on Automation Science and Engineering*, vol. 5, pp. 549-557, 2008.
- [5] M. Cole, and T. Wongratanaphisan, "A direct method of adaptive FIR input shaping for motion control with zero residual vibration," *IEEE/ASME Trans. on Mechatronics* vol. 18, pp.316-327, 2013.
- [6] I. M. S. Panahi, and K. Venkat, "A class of quadratic FIR shapers with applications to spectral shaping and narrow band generation," *Proc. of IEEE/SP 13th Workshop on Statistical Signal Processing*, Bordeaux, 2005, June 17-20, pp. 817-822.
- [7] M. Heertjes, and D. Bruijnen, "MIMO FIR feedforward design for zero error tracking control," *Proc. of American Control Conference (ACC)*, Portland, 2014, June 4-6, pp. 2166-2171.
- [8] B. R. Murphy, and I. Watanabe, "Digital shaping shapers for reducing machine vibration," *IEEE Trans. on Robotics and Automation* vol. 8, pp. 285-289, 1992.
- [9] M. R. Vander, T. Singh, and M. Steinbuch, "Time-delay pre-shaper design for vibration free tracking of periodic reference signals," *Proc. of American Control Conference (ACC)*, Chicago, USA, 2015, July 1-3, pp. 2167-2172.
- [10] W. Singhose, , W. Seering and N. C. Singer, "Shaping inputs to reduce vibration: a vector diagram approach," *Proc. of IEEE International Conference on Robotics and Automation*, Cincinnati, USA, 1990, May 13-18, pp. 922-927.

- [11] N. Singer, and W. Seering, "Pre-shaping command inputs to reduce system vibration," *ASME Journal of Dynamic Systems, Measurement, and Control* vol. 112, pp. 76-82, 1990.
- [12] W. E. Singhose, W. P. Seering, and N. C. Singer, "Shaping inputs to reduce vibration: a vector diagram approach," *Proc. of the IEEE International Conference on Robotics and Automation*, Brisbane, Australia, 1990, 21-26 May, pp. 922-927.
- [13] K. L. Sorensen, K. Hekman, and W. E. Singhose, "Finite-state input shaping," *IEEE Trans. on Control Systems Technology*, vol. 18, pp. 664-672, 2010.
- [14] W. Singhose, S. Derezinski, and N. Singer, "Extra-insensitive input shapers for controlling flexible spacecraft," *Journal of Guidance, Control, and Dynamics*, vol. 19, pp. 385-391, 1996.
- [15] M. J. Maghsoudi, Z. Mohamed, M. O. Tokhi, A. R. Husain, and M. S. Z. Abidin, "Control of a gantry crane using input-shaping schemes with distributed delay," *Trans. of the Institute of Measurement and Control*, DOI: 10.1177/0142331215607615 pp. 1-10, 2015. To be published
- [16] M. J. Maghsoudi, Z. Mohamed, A. R. Husain and M. O. Tokhi, "An optimal performance control scheme for a 3D crane," *Mechanical Systems and Signal Processing* vol. 66-67, pp.756-768, 2016.
- [17] Z. Mohamed, J. M. Martins, M. O. Tokhi, C. J. Sada, and M. Botto, "Vibration control of a very flexible manipulator system," *Control Engineering Practice*, vol. 13, pp. 267-277, 2005.
- [18] A. M. Abdullahi, Z. Mohamed, M. S. Zainal Abidin, S. Buyamin, and A. A. Bature, "Output-Based command shaping technique for an effective payload sway control of a 3D crane with hoisting," *Trans. of the Institute of Measurement and Control*, DOI: 10.1177/0142331216640871 pp. 1-11, 2016. To be published
- [19] L. Y. Jianqiang, Z. Dongbin, and W. Wei, "Adaptive sliding mode fuzzy control for a two-dimensional overhead crane," *Mechatronics* vol. 15, pp. 505-522, 2005.
- [20] Z. Mohamed, and M. O. Tokhi, "Hybrid control schemes for input tracking and vibration suppression of a flexible manipulator," *Proc. of the Institution of Mechanical Engineers, Part I: Journal of Systems and Control Engineering* 217:23-34, February 1, 2003.
- [21] K. Chul-Goo and H. Manh-Tuan, "Partially analytical extra-insensitive shaper for a lightly damped flexible arm," *Proc. of IEEE international conference on intelligent robots and systems*, Chicago, IL, USA, 2014, Sept. 14-18, pp.2401-2406.